U.S. DEPARTMENT OF COMMERCE
NATIONAL OCEANIC AND ATMOSPHERIC ADMINISTRATION
NATIONAL WEATHER SERVICE
NATIONAL METEOROLOGICAL CENTER

OFFICE NOTE 255

Practical Predictability

Joseph P. Gerrity, Jr.
David F. Parrish
Development Division

MAY 1982

1. Introduction

Practical predictability refers to the application of some of the techniques, used in the investigation of the classical predictability problem by Lorenz, Leith, and Smagorinsky, to the assessment of the operational performance of weather prediction models. The results produced may provide useful adjuncts to or extensions of NMC's standard diagnostic and verification programs.

In this paper, we present the results obtained in our preliminary investigations. Specifically, we show: some statistical intercomparisons of the spectral and LFM models; some indication of the greater differentiation of analysis differences admitted by comparing dynamically significant terms rather than just basic fields; some statistics on the growth of error in spectral model forecasts; and finally, some examples of pseudo-statistical dynamic forecasts.

2. Statistical Comparison of the LFM and Spectral Models

The LFM and Spectral models are routinely integrated twice each day. The forecasts produced by the models differ for a number of reasons. The data-base available is different because the forecasts are initiated at times that differ by about 2 hours. The more complete data set available to the Spectral model is analyzed by the use of Hough functions and is global in its extent. The LFM analysis is produced by the method of successive corrections and extends over only North America. Finally, of course, the model formulations of numerics and of physical processes differ in many ways.

In spite of the differences, outlined above, we generally find the model predictions to be largely in agreement. Recently, however, we have noted some marked departures between the forecasts. It is in part to address this fact that we have statistically computed the relationships shown by the

500 mb forecasts of the two models.

In figure 1 is shown the mean difference between the Spectral model and the LFM model forecasts of 500 mb height and wind speed, during two weeks in March 1982. The LFM model shows systematically larger wind speed but the magnitude of the difference is quite small. Except at the 48 hour forecast time the same properties are shown by the mean height difference.

Turning to figure 2 in which we show the standard deviation of the height and wind speed differences, we observe that, after an initial adjustment, the model's forecasts show a linearly increasing difference with time.

Figure 3 shows the evolution of the correlation coefficient between the predicted height, wind speed, relative vorticity and vorticity advection forecasts produced by the two models. The height field remains very highly correlated throughout the forecast period (48 hours). The other three parameters show some increase in correlation during the first twelve hours followed by a linear decline in correlation throughout the remainder of the forecast period.

It is especially noteworthy that the weather, or vertical velocity, related advection of relative vorticity term shows the most precipitous drop in correlation, to less than 0.5 by 48 hours. On the average therefore we may expect the user of the model forecasts to be faced with a difficult decision in reconciling the weather-related significance of the two forecasts. Certainly the provision of assistance in making these decisions should be a high priority for research and development.

3. Diagnostic Analysis Differences

It is often times difficult, through visual inspection of routine analysis maps, to draw any conclusions on the extent and significance of two separate analyses valid at the same time. An example of this fact is shown in figure 4, which shows the 250 mb height field analysis produced by the Hough function and successive correction analysis methods for 12Z 11 Feb 82. Especially over the data dense USA there are only minor differences in evidence.

The situation is somewhat less ambiguous in figure 5 which shows the two 250 mb relative vorticity analyses. The intensity of the vorticity maximum in Nevada is significantly greater in the LFM analysis, and we notice a pronounced difference over Mexico and south western Texas.

Figure 6 and 7 show for the Hough and LFM analysis, respectively, the kinetic energy and the generation term ($\mathbb{V} \cdot \nabla \phi$) at 250 mb. Again the LFM analysis shows generally greater intensity in both fields.

The conclusion seems evident that the diagnostic computation of quantities related to the wind analysis points out analysis differences more clearly than does a comparison of just the geopotential field. We have also examined the relationship between the 850-500 mb thickness field and the analyzed vertical shear of the wind, finding notable differences in the consistency of the analyses. Similarly, the patterns of relative vorticity advection at 500 mb have shown apparently important differences.

Having noted that one may diagnose significant model analysis differences, we must confess that we are not in a position to judge which of the two is more faithful to reality. We suspect that in many cases neither analysis can show the detail revealed by satellite imagery.

It does seem desirable, however, tedious and intractable the problem's investigation may be, to undertake the research needed to clarify the sensitivity of diagnostic dynamical quantities to the methods of analysis, and to clarify the impact of these differences upon forecast accuracy.

4. Spectral Model Error Growth

The central question addressed in classical predictability studies was the nature of the mechanisms responsible for the growth of forecast error. The significance of the spatial scale of disturbances for their predictability was empirically evident, and Lorenz early-on focused attention on the importance for predictability of the presence of a broad spectrum of spatial scales in the atmospheric circulation. Since the comprehensive observation of small scales is precluded by the practical limits of observing systems, current analysis-forecast systems ordinarily invoke one or another technique to filter out smaller scale components of the circulation. Thus, if it is true that the evolution of the unresolved scales is ultimately important for the evolution of larger scales, then the atmosphere is fundamentally unpredictable. The non-linearity of the equations of motion and the absence of a conclusive proof that a spectral-gap exists support the conclusion that, quite apart from the influence of sun, ocean and lithosphere, the atmospheric fluid has at best a limited range of predictability. The question then turns upon the rapidity with which the inevitable error grows and whether or not the possible forecast accuracy at a given time range is of practical utility.

The development of a global observational capability and the development of stable numerical methods for numerically solving the global meteorological equations have allowed us to undertake the production of objective forecasts into the medium-range, i.e. beyond 3 days. At NMC we now use the spectral model to produce forecasts to ten days. Since this prediction model uses the spectral method, it is relatively easy to examine its forecast skill in so-called phase space. While such examination of the forecasts is not a comprehensive diagnostic tool, it is uniquely capable of resolving forecast skill on the basis of the spatial scale of the atmospheric circulation.

We have initiated an investigation of the loss with time of forecast accuracy as a function of spatial scale. The spectral model uses as its basis functions the surface spherical harmonics $Y_n^m(\lambda, \phi)$ which are eigensolutions of the laplace operator in spherical coordinates, i.e.

$$\nabla^2 Y_n^m = -\frac{n(n+1)}{a^2} Y_n^m$$

The integer n is a measure of the scale of the function (n.b. a stands for the radius of the earth which is presumed to be approximately spherical.) By analogy to cartesian geometry for which

$$\nabla 2eikx = -k2eikx$$

with k the wave number, one has

$$n(n+1) = +k^2 a^2$$

The wave number k may be replaced by its value in terms of wave length L

$$k = \frac{2\pi}{L}$$

$$n(n+1) = \left(\frac{2\pi a}{L}\right)^2$$

Thus

$$L = \frac{(2\pi a)}{[n(n+1)]^{1/2}}$$

and some typical values of L for different n are given below using 6371 km for a.

n	L (km)	n	L (km)
1	28306		
2	16342	15	2584
3	11556	20	1953
4	8951	25	1570
5	7308	30	1313
6	6177	35	1128
7	5349	40	988
8	4718	45	880
9	4220	50	793
10	3817	55	721
		60	661

The other integer index m, used with the spherical harmonic Y_n^m is referred to as the zonal wave number. The function Y_n^m may be expanded into trigonometric functions of longitude $e^{im\lambda}$ and associate Legendre functions of latitude $P_n^m(\phi)$, i.e.

$$Y_n^m(\lambda, \phi) = e^{im\lambda} P_n^m(\phi)$$

The index m tells one how many zeroes of the function one encounters (2m) as one passes around a parallel of latitude. The difference (n-m) tells one how many zeroes one encounters is passing from pole to pole along a meridian. Only the zonal harmonics, for which m=0, are non-zero at the two poles. Thus if $m \neq 0$ the two pole zeroes must be added to (n-m) to obtain a total count of zeroes if one counts the polar zeroes.

Provided that one remains within a narrow band of latitude the zonal wave number offers a measure of scale of the associated wave perturbation, but the index m fails to be uniquely associated with the spatial scale over the full globe. Only the index n is a homogeneously valid measure of spatial scale over the spherical surface. Therefore we use the index n in the following figures displaying the growth of forecast error.

At the present time, the predicted wind field is archived only for 72 hours, consequently we have focused on the geopotential height at various pressure levels as a measure of forecast accuracy. For purposes of ground-truth the analyzed height field is used as produced by Flattery's Hough function method. The resolution afforded by the analysis extends to zonal wave number 24 and is rhomboidal. The Hough functions are represented analytically by infinite series of surface spherical harmonics. For use with the spectral model the spherical harmonic series is truncated at $n=|m|+30$ which has the upper bound $n=|24|+30=54$ since $|m|\leq 24$ for the Hough analysis fields. Tests have shown that the analysis is well represented by the truncated series of surface spherical harmonics.

To explain the graphs which follow assume that the series representing the height field is

$$z(\lambda,\varphi) = \sum_{m=-J}^{+J} \sum_{n=|m|}^{|m|+J} Z_{m,n} Y_n^m(\lambda,\varphi)$$

The coefficients $Z_{m,n}$ are complex numbers and since z is real the coefficients satisfy the condition

$$z_{-|m|,n} = Z^{*}_{|m|,n}$$

where the asterisk denotes the complex conjugate.

The rhomboidal truncation at J=30 may be shown graphically as in figure 10. For a given value of n less than J+1 there are (2n+1) coefficients $Z_{m,n}$; for $n\geq J+1$ there are $4J-2(n-1)$ coefficients $Z_{m,n}$ in the series. For each value of m the series contains the same number of terms; the same is true for each unique value of $n-|m|$.

The total variance of the field z is

$$\sigma^2 = \frac{1}{4\pi}\int_0^{2\pi}\int_{-\pi/2}^{\pi/2} z^2 \cos\phi \, d\lambda \, d\phi - Z_{0,0}^2$$

and because of the orthogonality of the Y_n^m,

$$\sigma^2 = 2\sum_{m=0}^{J} \sum_{n=m}^{m+J} \left(Z_{m,n} Z^{*}_{m,n}\right) - 2 Z_{0,0}^2$$

The coefficient $Z_{0,0}$ is the mean value of Z.

In figures 12 through 15 we show a comparison between the persistance error, the spectral model forecast error and the verifying analysis for 1, 2, 4, and 8 day forecasts all verifying on April 15, 1982.

In figure 12 (one day forecasts) the value of a prediction model stands out in the intermediate scales for which $7 \le n \le 24$. Not only is the model forecast error less than persistance but it is also appreciably less than the analyzed spectral density. Only for waves n=1 and 2 does the forecast model fare worse than the persistance forecast, however the distinction seems trivial since both errors are very small.

In figure 13 (two day forecast) the picture is more or less the same except that spectral density of the model forecast error has been degraded for waves beyond about n=17. We may also note that model forecast for waves 3 and 5 have improved in comparison to the persistance forecasts.

In figure 14 the four day forecast error spectra are shown. The forecast model now does better than persistance for wave n=2. The forecast error spectral density is less than the analysis for waves $n \le 8$ with the exception of n=5. For larger wave numbers predictive skill has been lost by four days.

Finally in figure 15, the 8 day forecasts are shown. The prediction model does less well than persistance for the very long waves n=1 and 2, and for n greater than 4 predictive skill may be said to have been lost, since the error spectral density exceeds that of the analysis.

5. Pseudo-Statistical Dynamic Forecasts

We have noted above that the forecasts produced by the spectral and LFM models proceed from different analyses and evolve in fashions that are systematically different. A practical problem then appears to warrant serious consideration viz., how should the information contained in the two forecasts

The spectral power density per total wave number S_n may be defined by

$$S_n = \frac{1}{n+1/2} \sum_{l=0}^{n} \left(z_{l,n} \, z_{l,n}^{*} \right) \qquad 0 \le n \le J,$$

and

$$S_n = \frac{1}{2J+1-n} \sum_{l=n-J}^{J} \left(z_{l,n} \, z_{l,n}^{*} \right) \qquad J+1 \le n \le 2J.$$

When plotting the spectral power density of the forecast error we use the representation

$$z^{E}_{m,n} = z^{F}_{m,n} - z^{A}_{m,n}$$

where $z^{F}_{m,n}$ is the forecast coefficient, $z^{A}_{m,n}$ is the verifying analysis coefficient and $z^{E}_{m,n}$ is the error field coefficient.

In the following graphs we plot the $\log_{10} S_n$ versus n on a logarithmic scale. The material shown here is just a sampling of the results so far obtained. We plan to do additional analysis and will report more comprehensively at a later time.

In figure 11, we show the spectrum of the 500 mb height analysis valid on 15 April 1982 as the heavy line. Also shown are the error spectra of persistance forecasts made 1, 2, 4 and 8 days prior to the verifying analysis. These errors of persistence provide an indirect indication of the temporal variability of the 500 mb height field. The error is contributed by both amplitude and phase differences between the forecast (persistance in this case) and verifying analysis.

The persistance forecast error spectral density reaches levels comparable to that in the analysis for total wave number $n \geq 10$ within one day. For waves with $n \leq 4$ the persistance error density is quite small compared to the analysis spectral power density. For waves with $n \geq 5$, persistance forecasts possess error levels comparable to or greater than the analysis by 4 days.

be distilled into a unique set of guidance for the forecaster.

If one possessed an adequate statistical basis on which to construct a statistically optimal combination of the two forecasts one could procede as outlined in the appendix. Absent that information, we may simply average the forecasts and interpret their departures from each other as a measure of the forecast uncertainty. Such an operation could be readily exercised using mini-computers available to the NWS field offices.

As a very preliminary example we have chosen the case of 19 Mar 82, in which the LFM and spectral models produced widely different forecasts of a lee-cyclogenesis. The 48, 36 and 24 hour forecasts of 500 mb height from the spectral and LFM models valid at 12Z 19 Mar 82 were averaged together and the standard deviation from this mean computed. The result is shown in figure 8. The large difference in the forecasts is readily evident in the 100 m central value of the standard deviation found over Kansas.

In figure 9 we show the analysis of the observed 500 mb height field and the error of the mean forecast. It is encouraging to note that the mean forecast error is highly correlated to the estimate of uncertainty provided by the standard deviation field in figure 8.

The production of pseudo-statistical dynamic forecasts is not a substitute for the production of more accurate deterministic forecasts, but it does recognize, in some measure objectively, the level of uncertainty faced by the forecasters who must interpret numerical model forecasts.

Appendix: Optimal Forecast Formulation

Suppose that one has a set of forecasts, all valid at the same time, which were produced in a variety of ways. How should one combine these forecasts into an optimal forecast, i.e. one which in the ensemble average has the least square error? A related question is, how to obtain an estimate of the probable error of the optimal forecast?

Let z_i represent the set of N forecasts and let z represent the optimal linear combination of those forecasts

$$Z = \sum_{i=1}^{N} w_i Z_i \tag{1}$$

where w_i is a set of weights. The error of the optimal forecast may be expressed by e

$$e = Z - \hat{Z} \tag{2}$$

where $\hat{Z}$ is the true field at the verifying time.

The forecast Z is statistically optimal if we select the coefficients w_i so that in the ensemble average, denoted by $\overline{(\ )}$, the value $\overline{(e^2)}$ is a minimum. That is we require

$$\frac{\partial}{\partial w_i} \overline{e^2} = 0 \quad ; \quad i = 1, 2, \ldots, N. \tag{3}$$

If we define the N by N matrix C to have the elements

$$c_{ij} = \overline{z_i z_j} \tag{3}$$

and define the vectors $\underline{w}$ and $\underline{x}$ by

$$\underline{w} = (w_i)^T \tag{4a}$$

$$\underline{x} = (\overline{\hat{z} z_i})^T \tag{4b}$$

The weights $\underline{w}$ satisfying the optimality condition (2) are given by

$$\underline{w} = H \bar{\underline{x}} \tag{5}$$

with

$$H = C^{-1} \tag{6}$$

The expected value of the forecast error e will be zero, provided that

$$\sum_i w_i \bar{z}_i = \bar{\hat{z}} \tag{7}$$

The right hand side term in 6 will be zero, if we define the forecast problem as being the prediction of departures from some ensemble mean, rather than the prediction of the entire field. To do the problem in such terms would require that the prediction model be free of bias, i.e. be free of the so-called climate drift error. In the optimal system outlined above we should certainly require a knowledge of both $\bar{\hat{z}}$ and $\bar{z}_i$, and consequently the removal of $\bar{z}_i$ and $\bar{\hat{z}}$ from the problem's statement requires no significant additional effort, when compared to the computation of the matrix C and the vector $\underline{x}$. Thus we must turn to the expected value of e^2 to define a measure of the error associated with a statistically optimal forecast.

The expected ensemble mean square error is

$$\overline{e^2} = \overline{(z - \hat{z})^2} = \overline{\hat{z}^2} - \overline{\left[2 \langle H\bar{\underline{x}}, \underline{z} \rangle \hat{z} - \langle H\bar{\underline{x}}, \underline{z} \rangle^2 \right]}$$

Provided the quantity in braces is positive the statistically optimal forecast will reduce $\overline{e^2}$ below the ensemble climate variance $\overline{\hat{z}^2}$. This is the "tempered" forecast aspect of statistically optimized forecasts which is not shared by completely deterministic forecasts which in the limit of zero correlation yield expected forecast error variance twice that of the ensemble climate variance. The use of $\underline{HX}$ for the weighting of the several deterministic forecasts insures that we minimize $\overline{e^2}$, and at least, in principle, the expected mean square error will be less than the ensemble climatological variance.

It is of course a considerable undertaking to estimate the required statistics for a sufficiently large sample to be representative of the ensemble of all possible realizations. Approximations of the mathematically complete problem will be necessary.

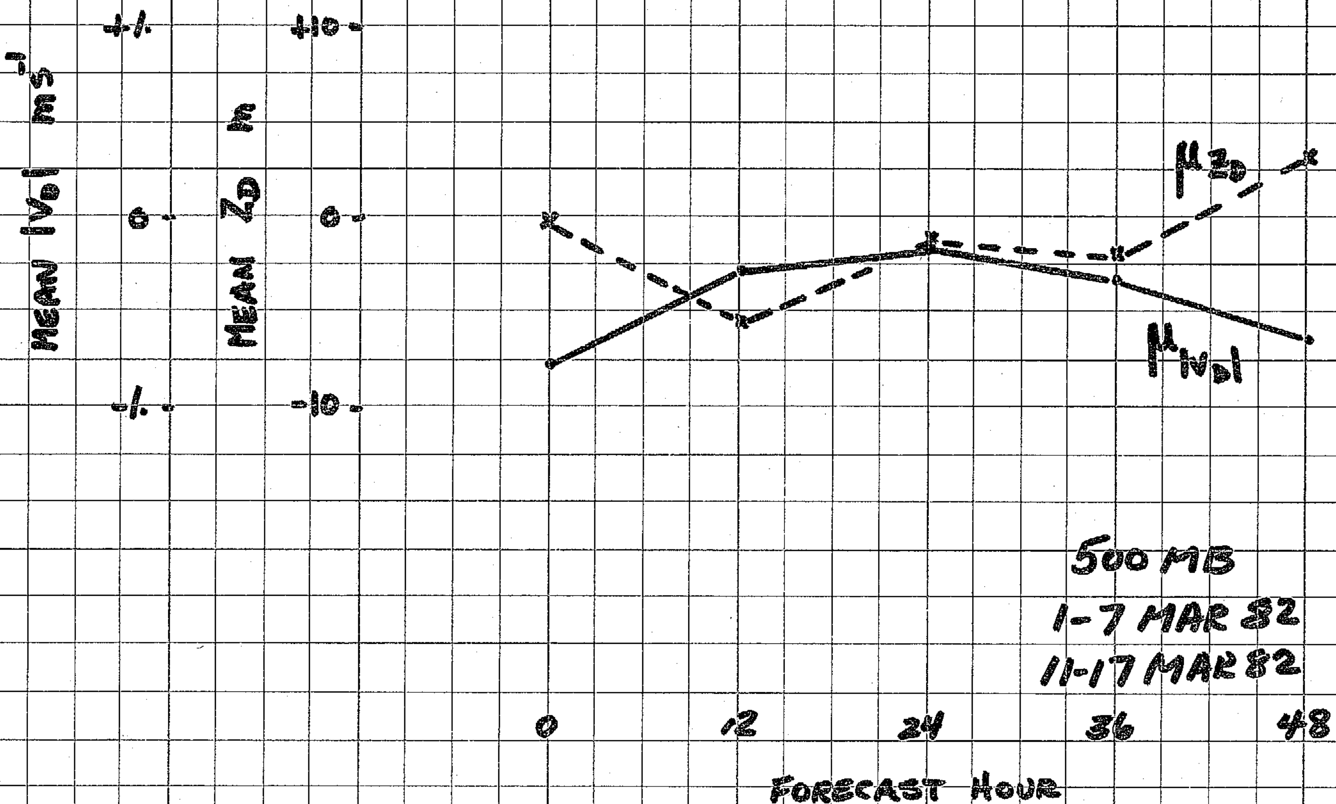

MEAN |V_D| m s^-1
MEAN Z_D m
+1.
0
-1.
+10
0
-10
μZD
μ|VD|
500 MB
1-7 MAR 82
11-17 MAR 82
0
12
24
36
48
FORECAST HOUR

FIG 1

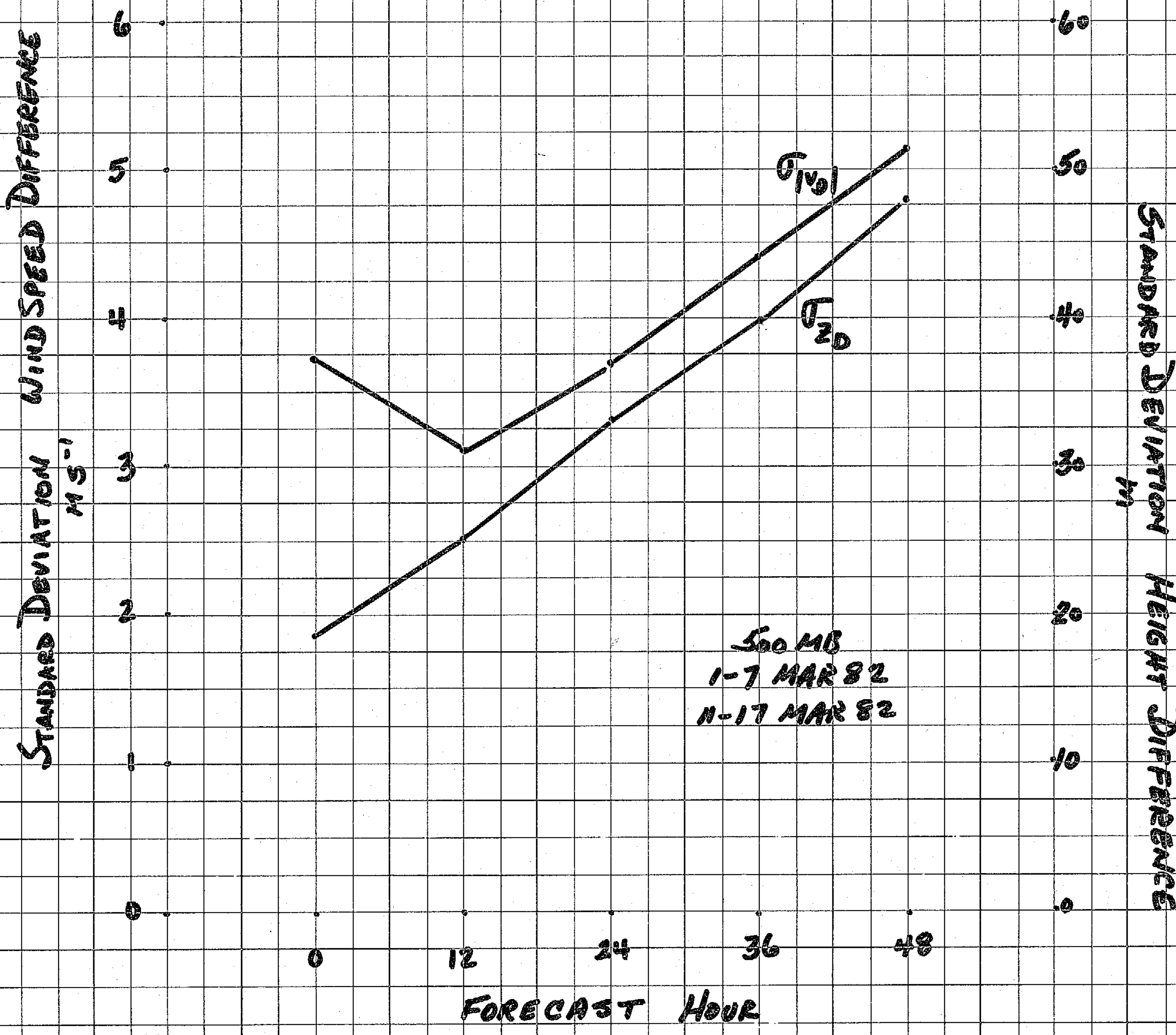
STANDARD DEVIATION WIND SPEED DIFFERENCE
M S⁻¹
STANDARD DEVIATION HEIGHT DIFFERENCE
M
6
5
4
3
2
1
0
60
50
40
30
20
10
0
0
12
24
36
48
FORECAST HOUR
$\sigma_{|V_D|}$
σ_{Z_D}
500 MB
1-7 MAR 82
11-17 MAR 82

FIG. 2.

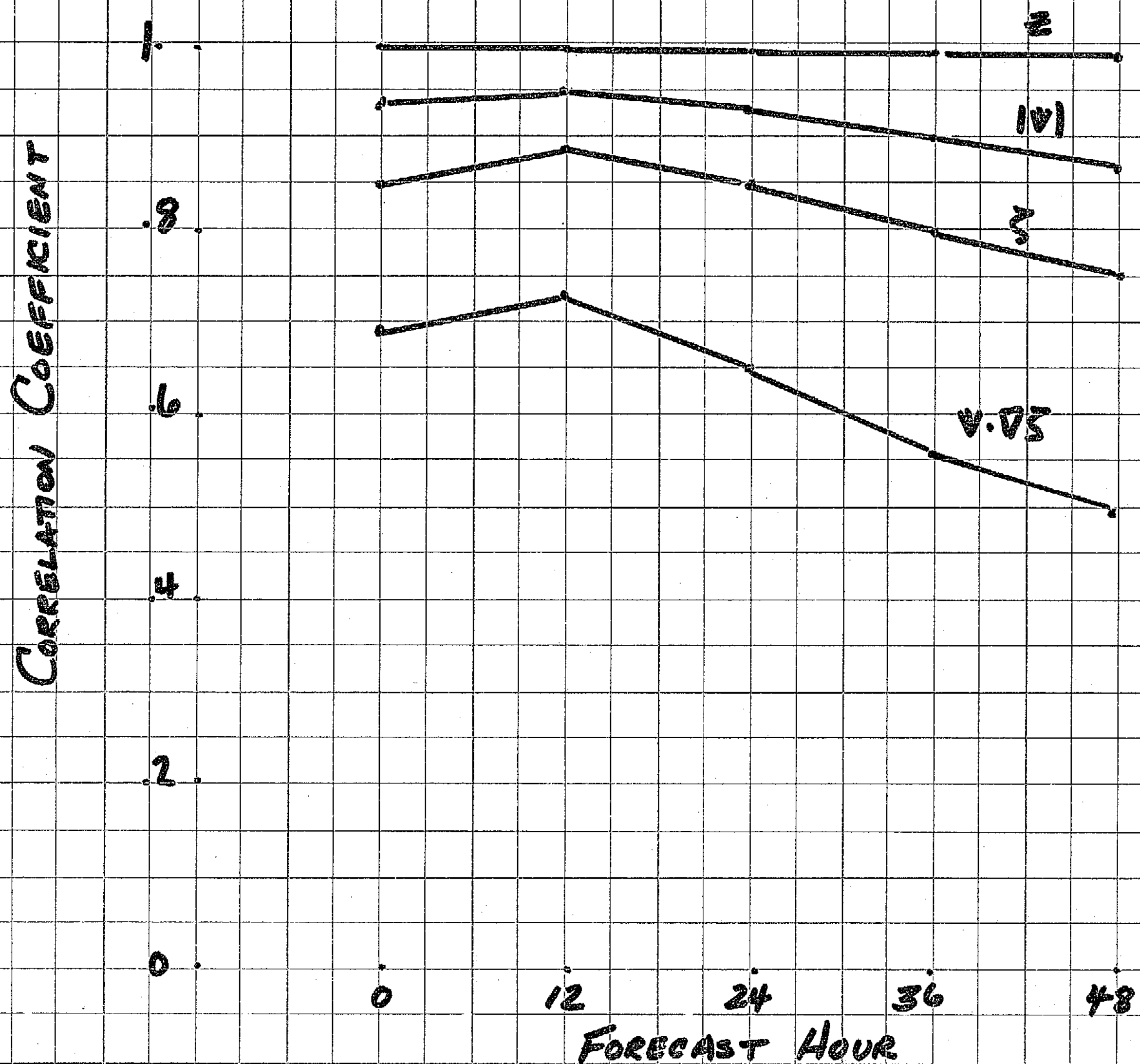

Correlation Coefficient
1.
.8
.6
.4
.2
0
0
12
24
36
48
Forecast Hour
z
|V|
ζ
V·∇ζ

FIG. 3

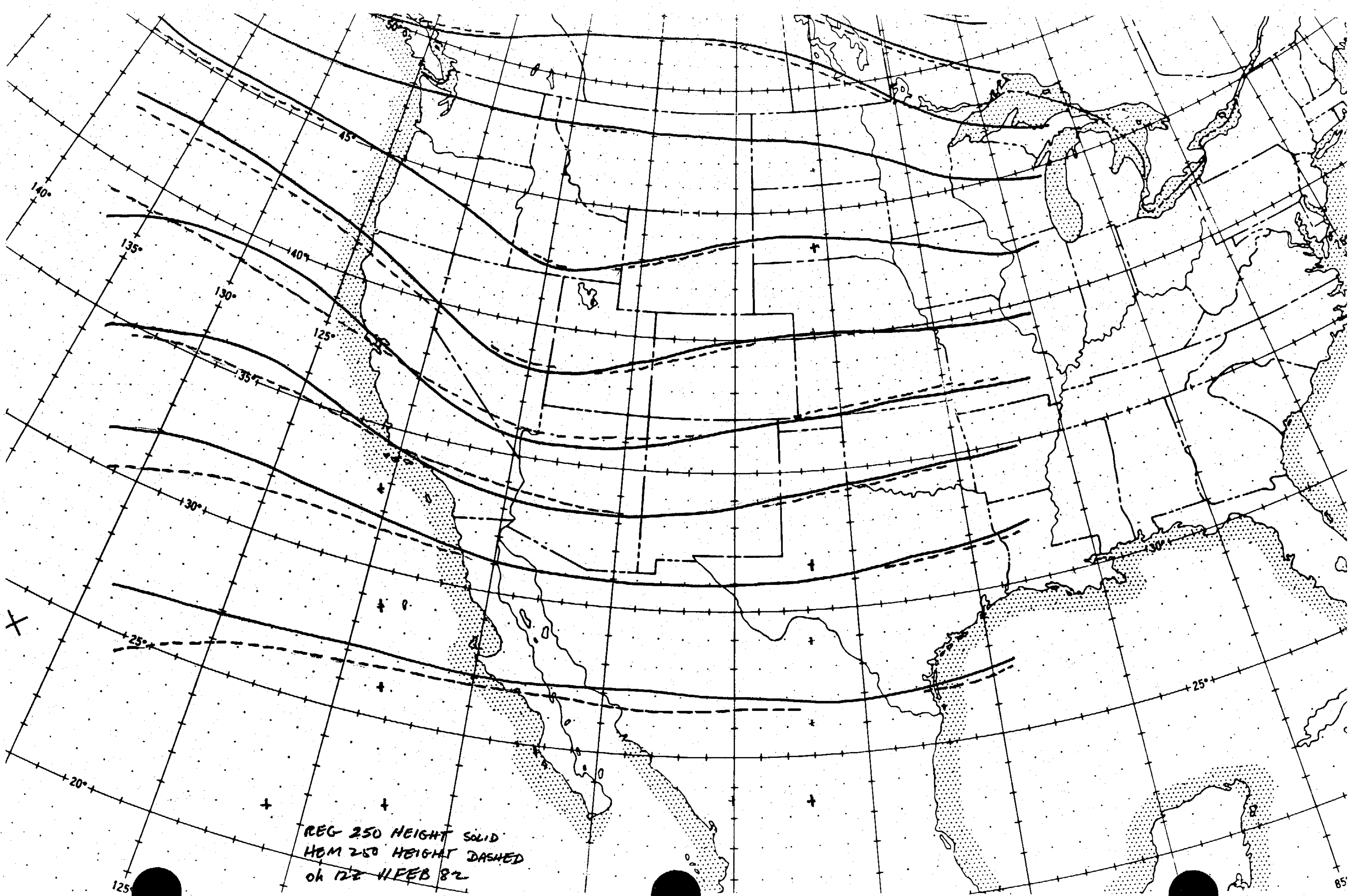

REG 250 HEIGHT SOLID
HEM 250 HEIGHT DASHED
0h 12Z 11FEB 82

Fig 4.

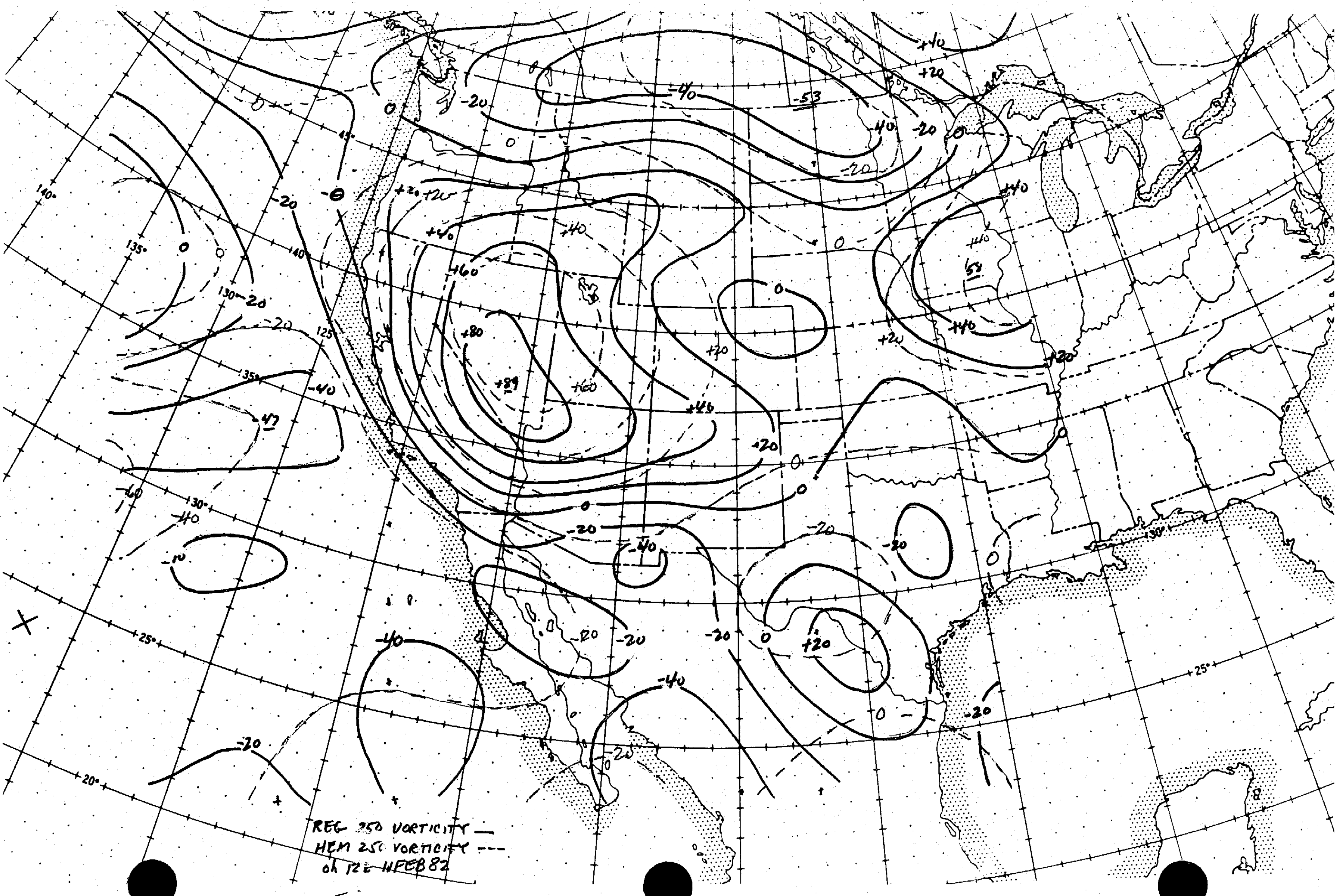

Fig 5.

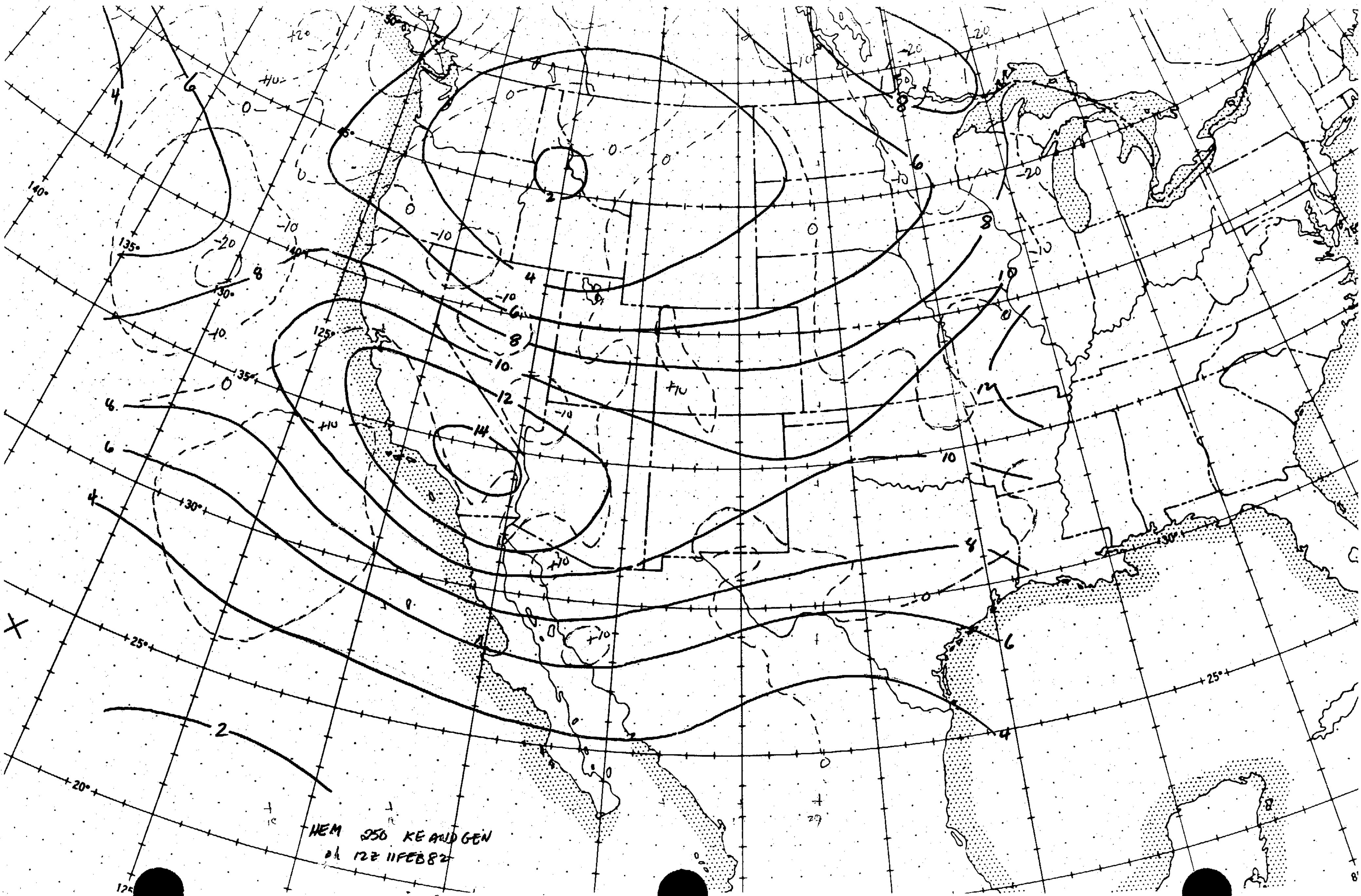

Fig 6

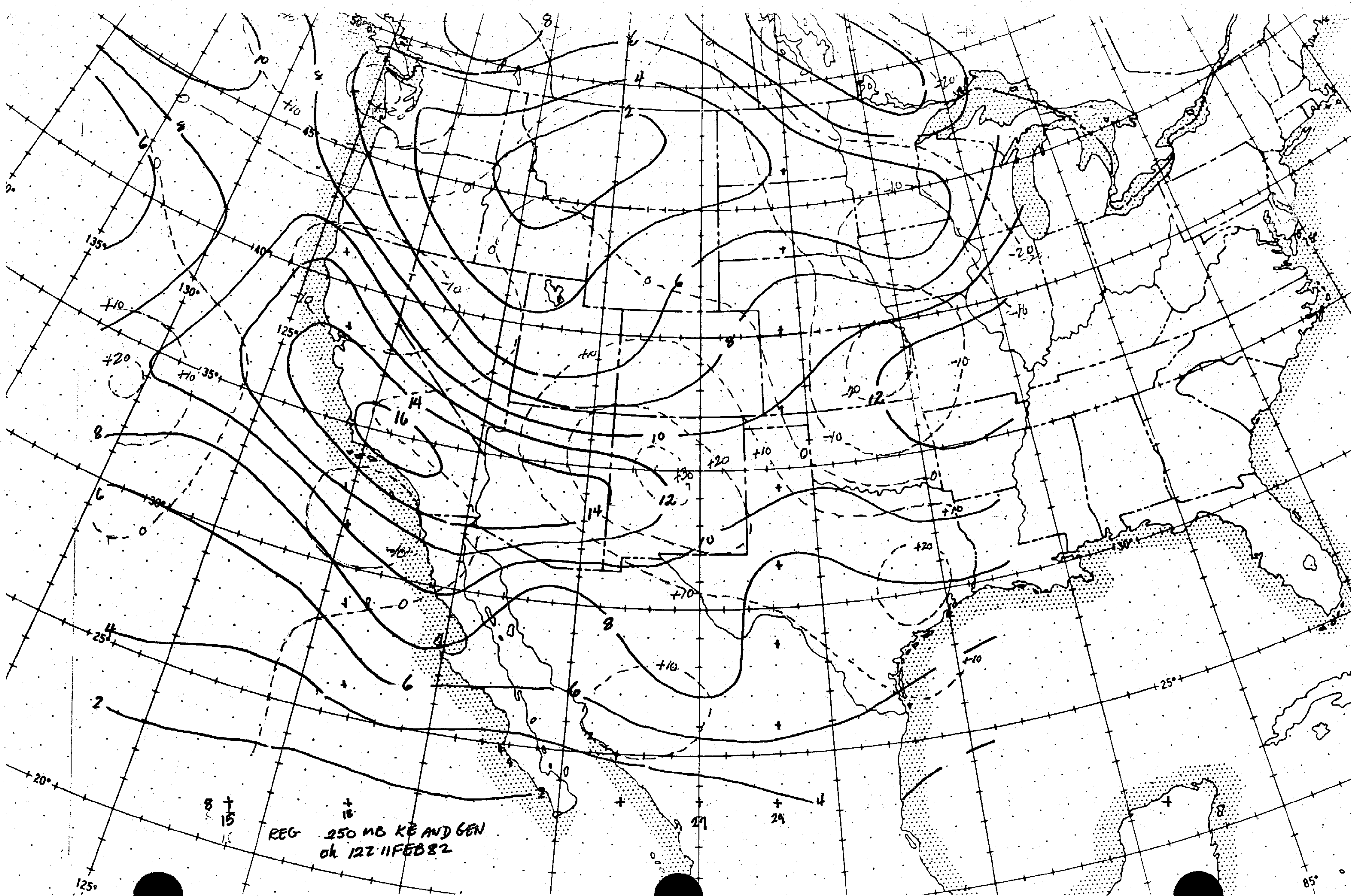

Fig 4.

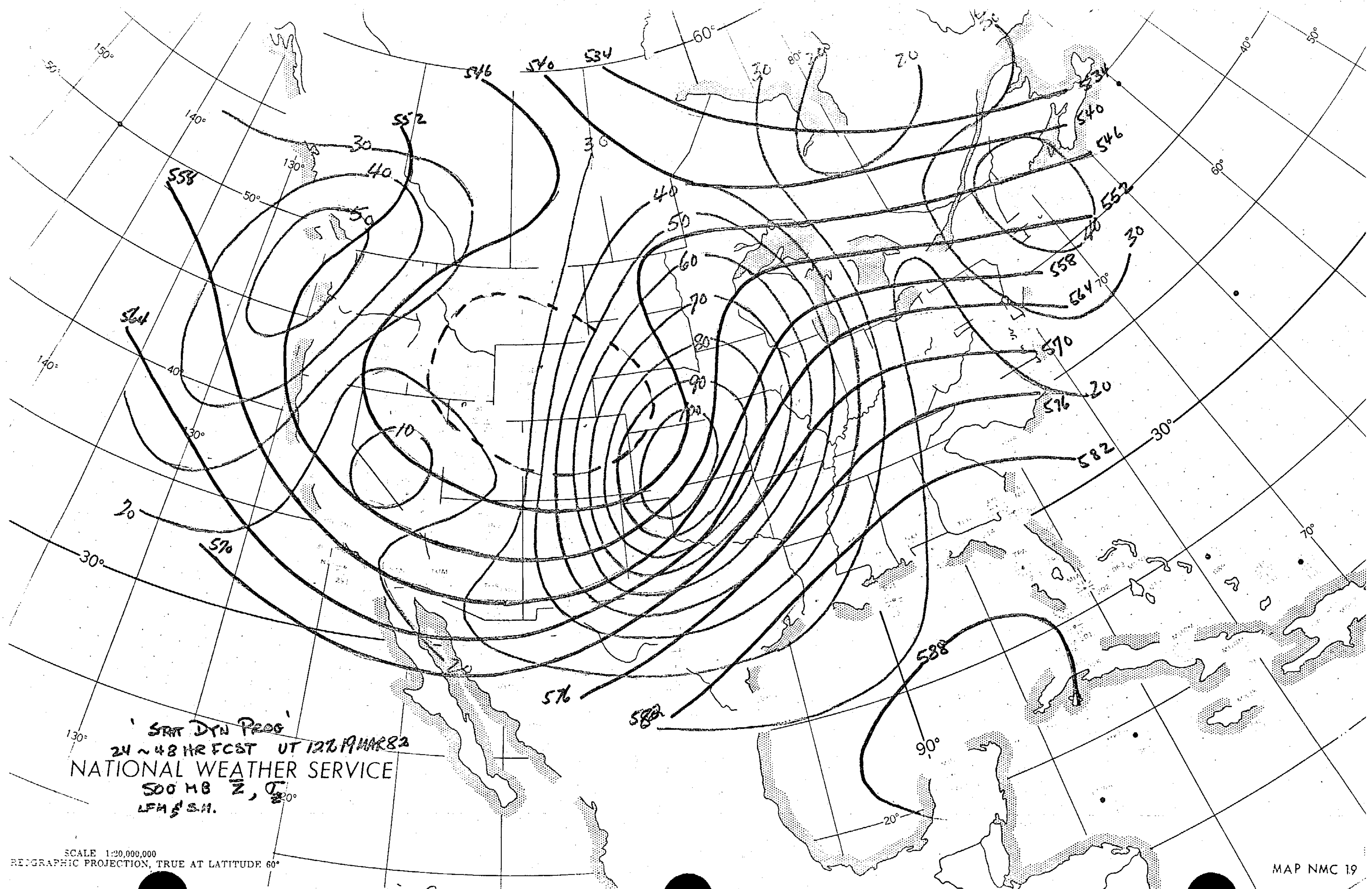
'STAT DYN PROG'
24 ~ 48 HR FCST UT 12Z 19MAR82
NATIONAL WEATHER SERVICE
500 MB Z, ζ
LFM & S.H.
SCALE 1:20,000,000
REOGRAPHIC PROJECTION, TRUE AT LATITUDE 60°
MAP NMC 19

Fig 8

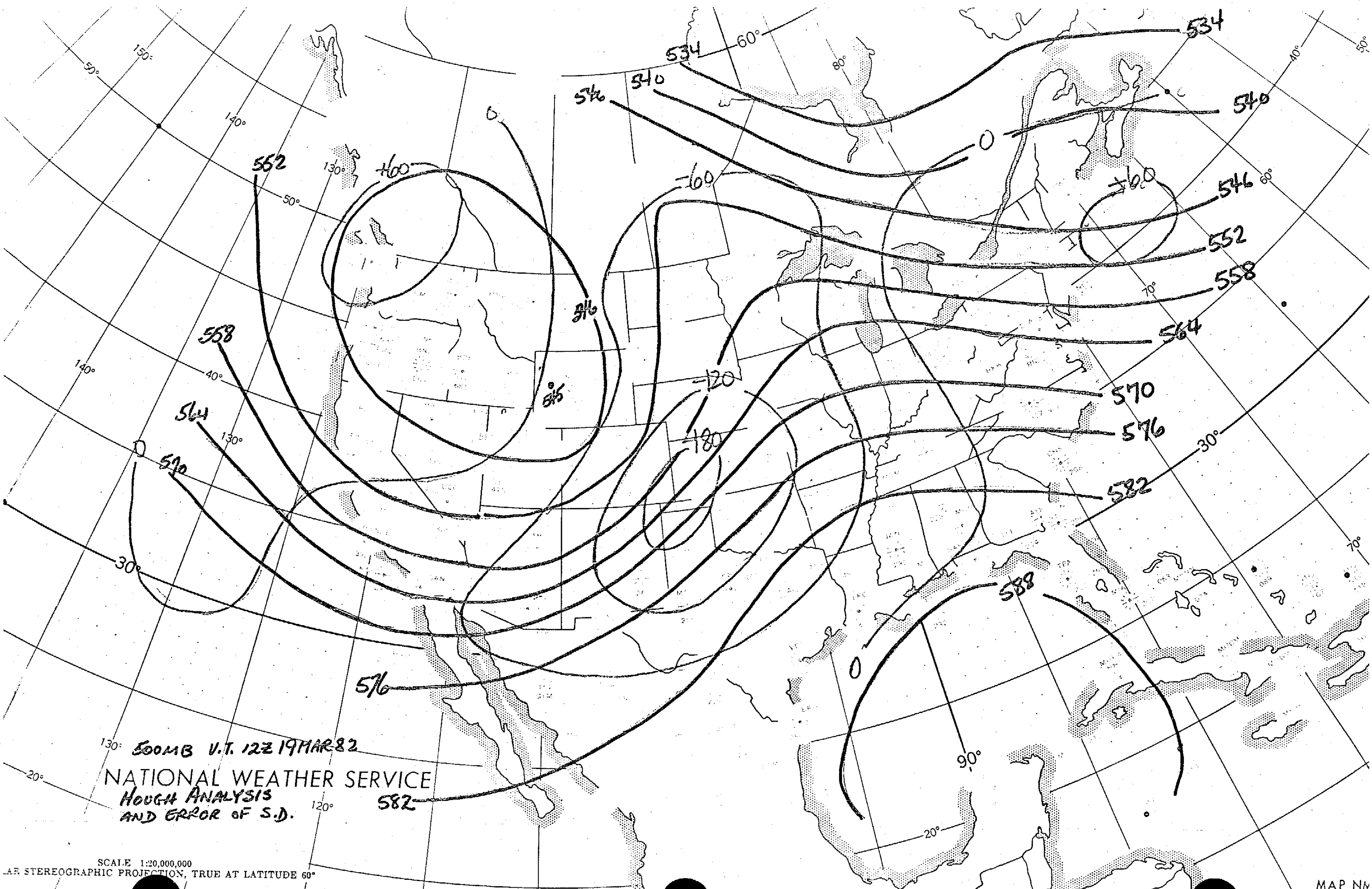
500MB V.T. 12Z 19MAR82
NATIONAL WEATHER SERVICE
HOUGH ANALYSIS
AND ERROR OF S.D.
SCALE 1:20,000,000
AR STEREOGRAPHIC PROJECTION, TRUE AT LATITUDE 60°
MAP NM
534
540
546
552
558
564
570
576
582
588
+60
-60
-120
-180
0

Fig 9.

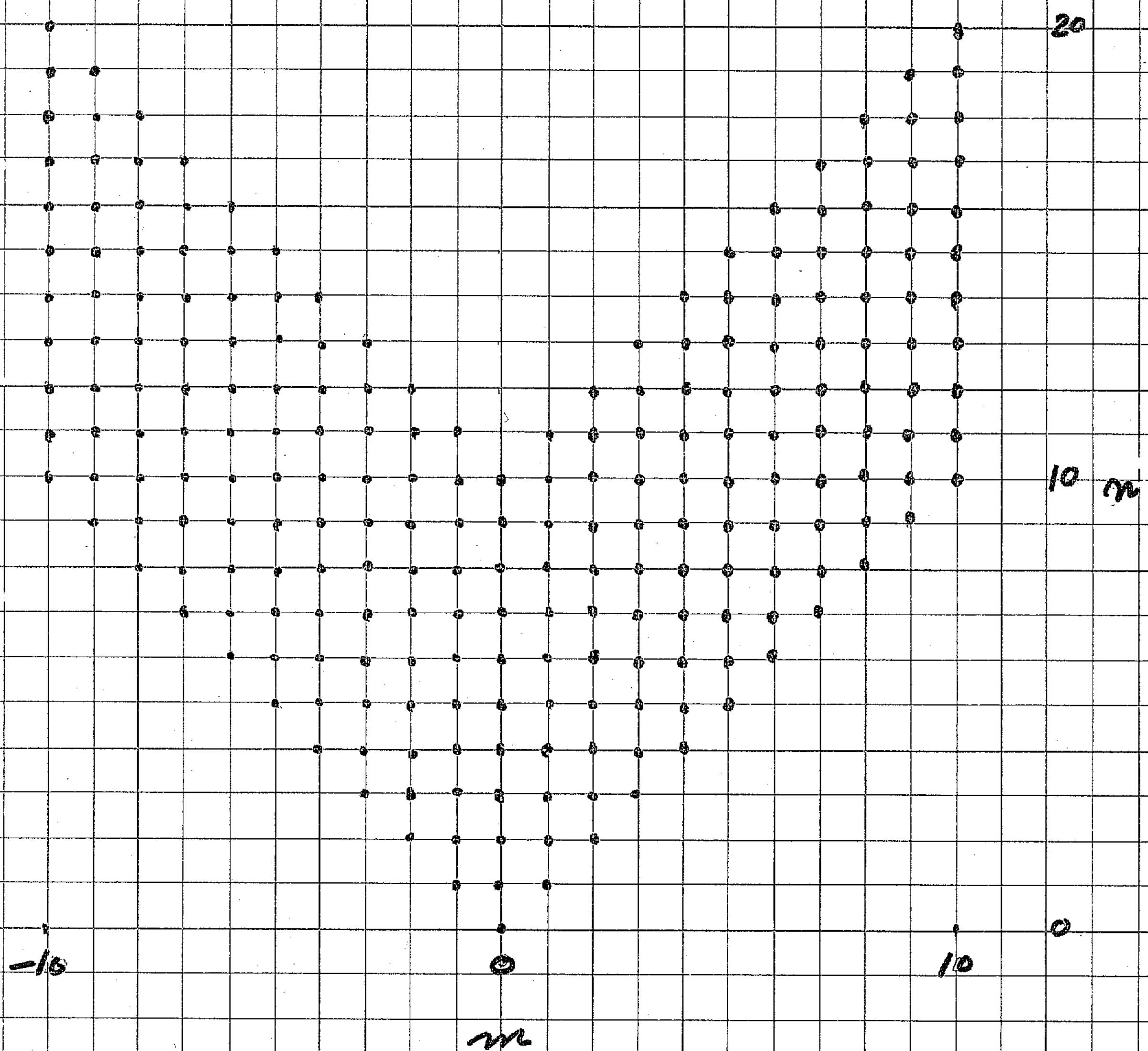

FIG. 10 LATTICE OF COEFFICIENTS FOR RHOMBOIDAL TRUNCATION, J=10.

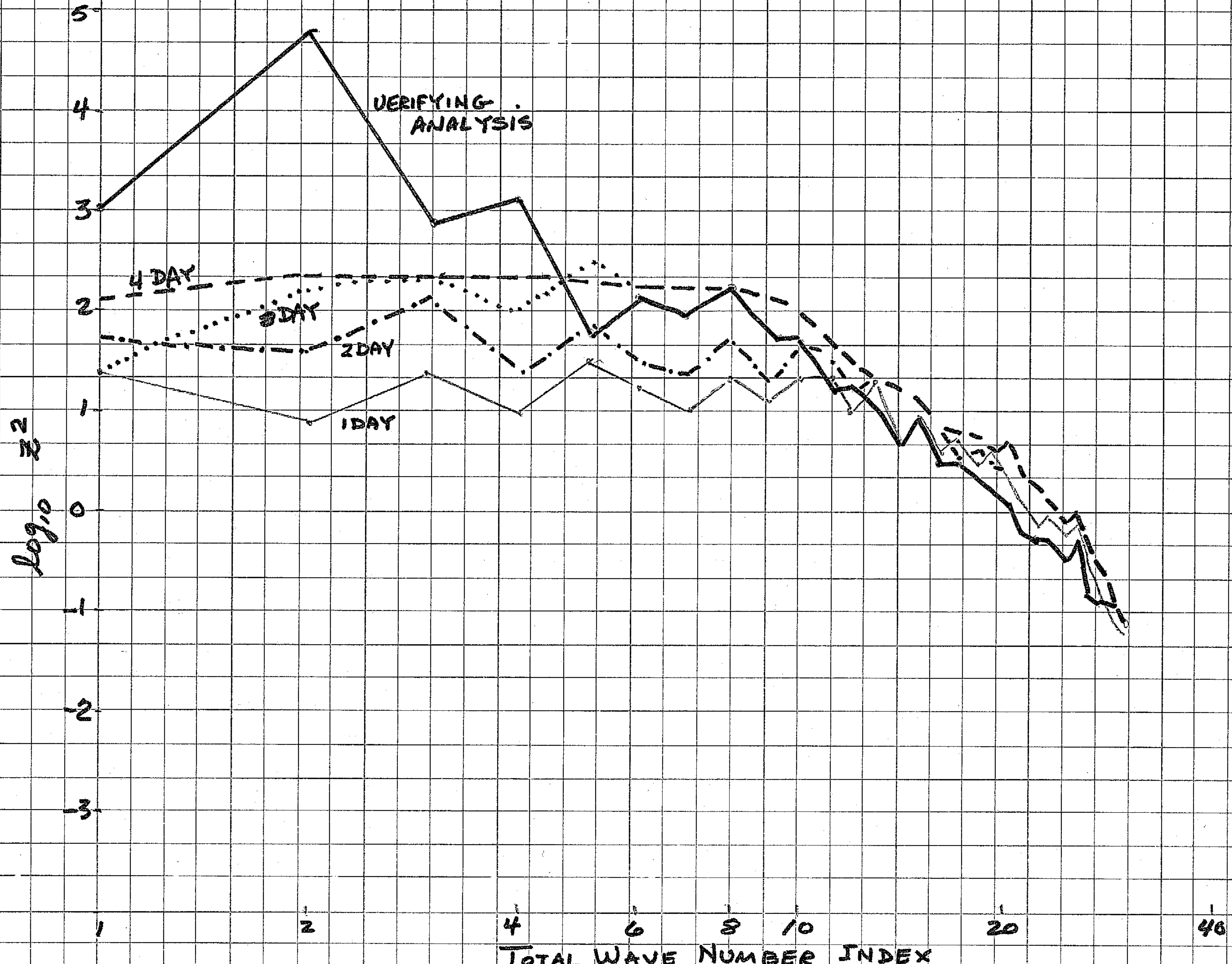

FIG 11 PERSISTANCE FORECAST ERROR

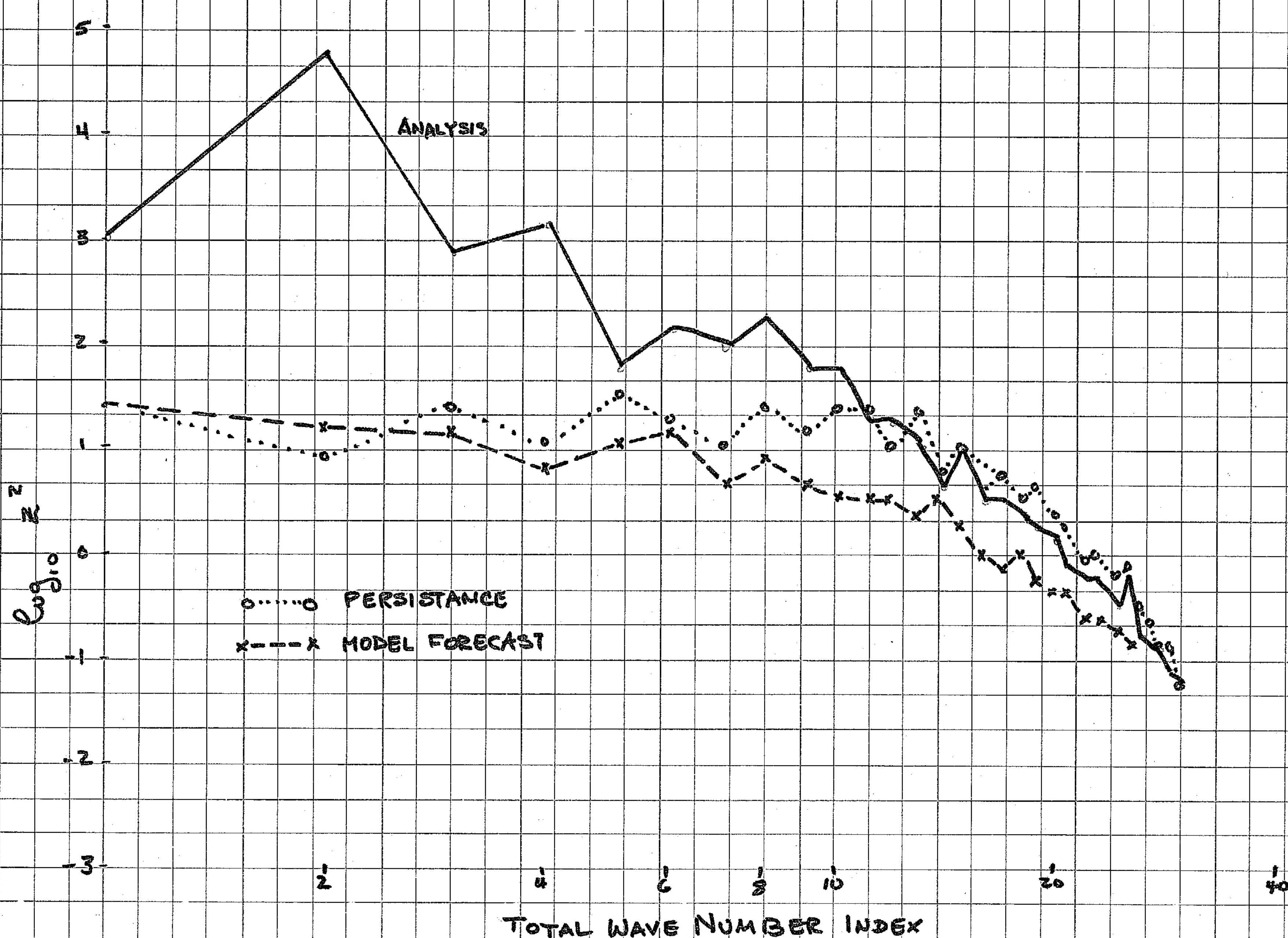

FIG 12 24 HR FORECAST ERROR

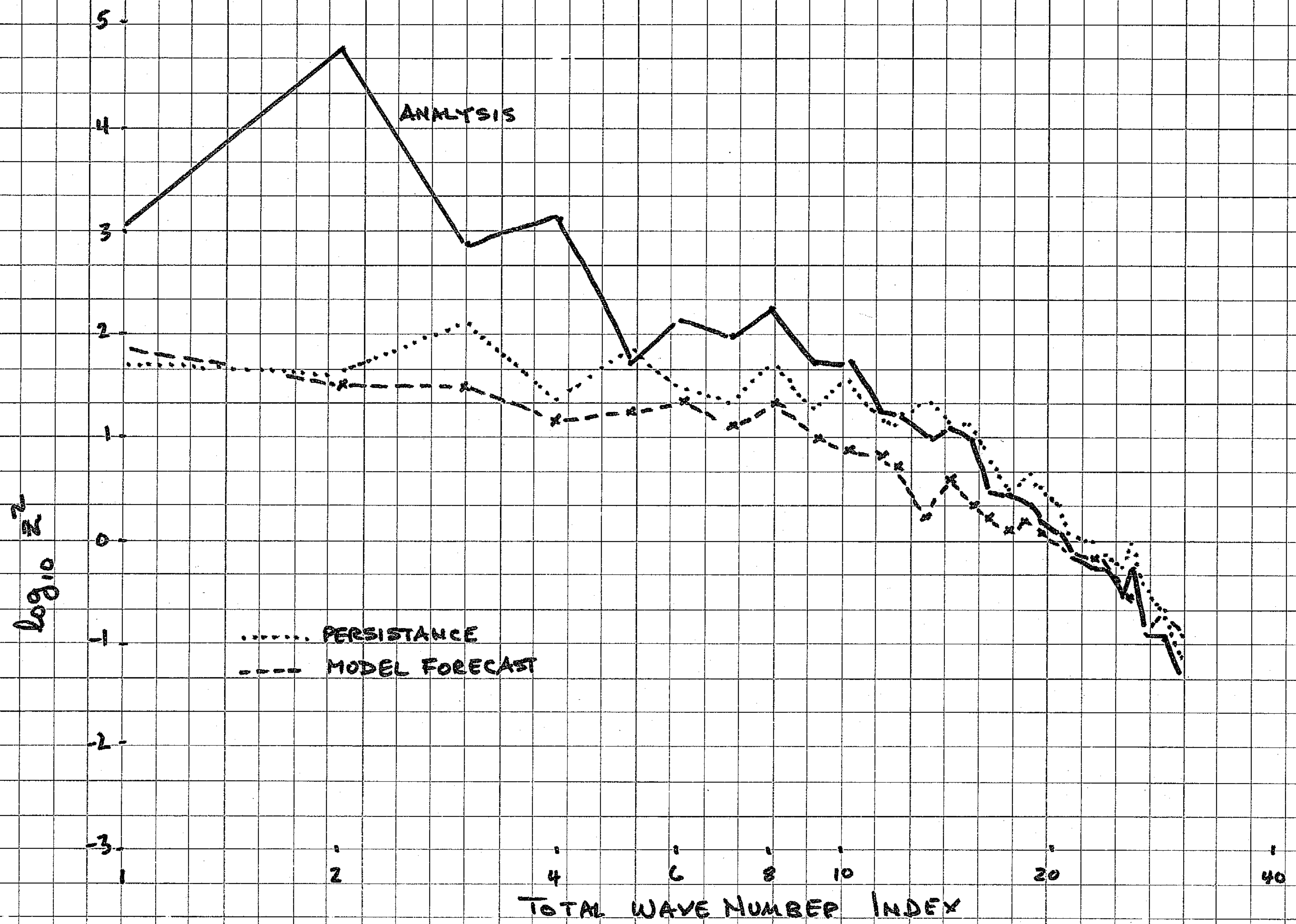

FIG 13. 48 HR FORECAST ERROR

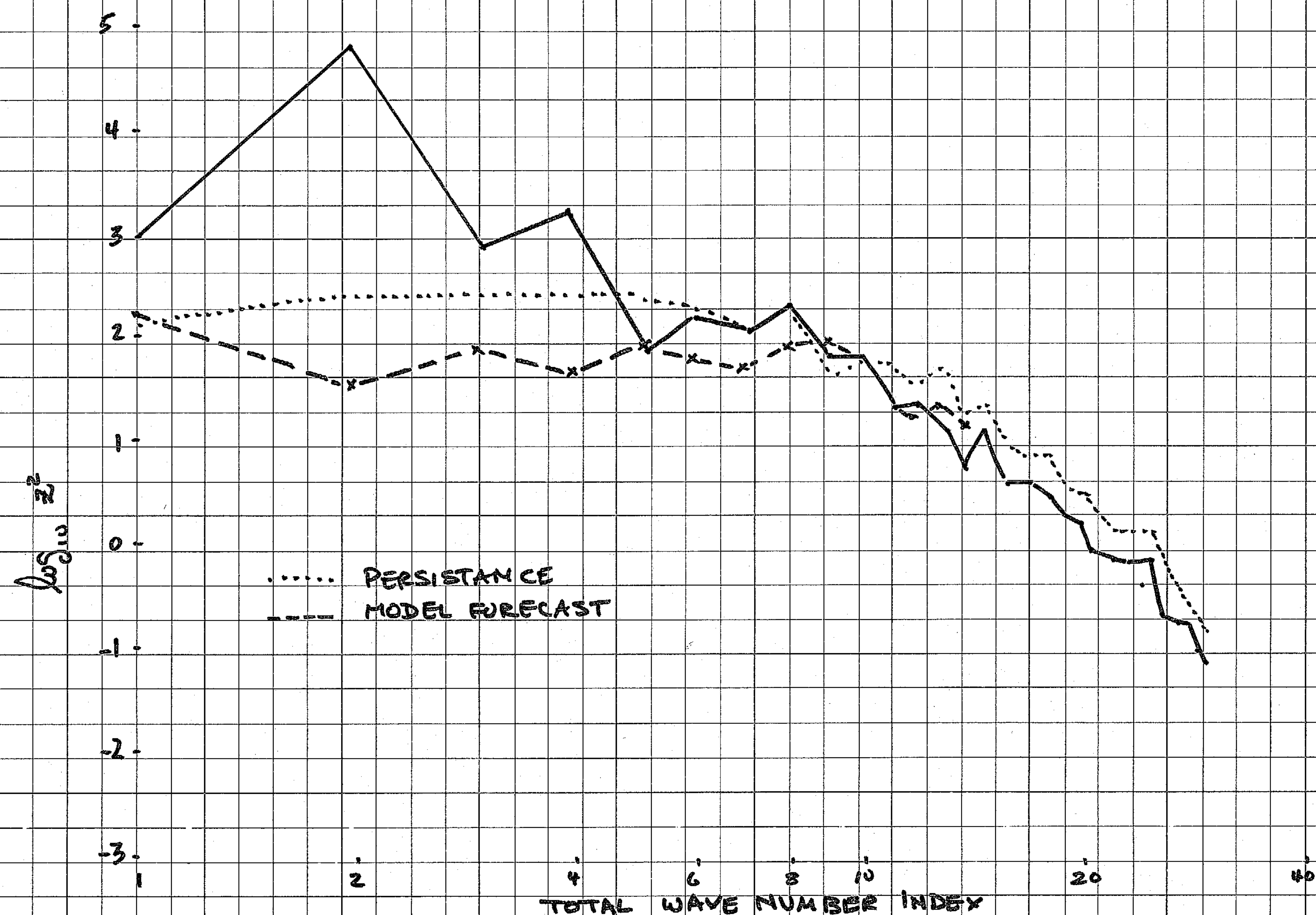

FIG14 96 HOUR FORECAST ERROR

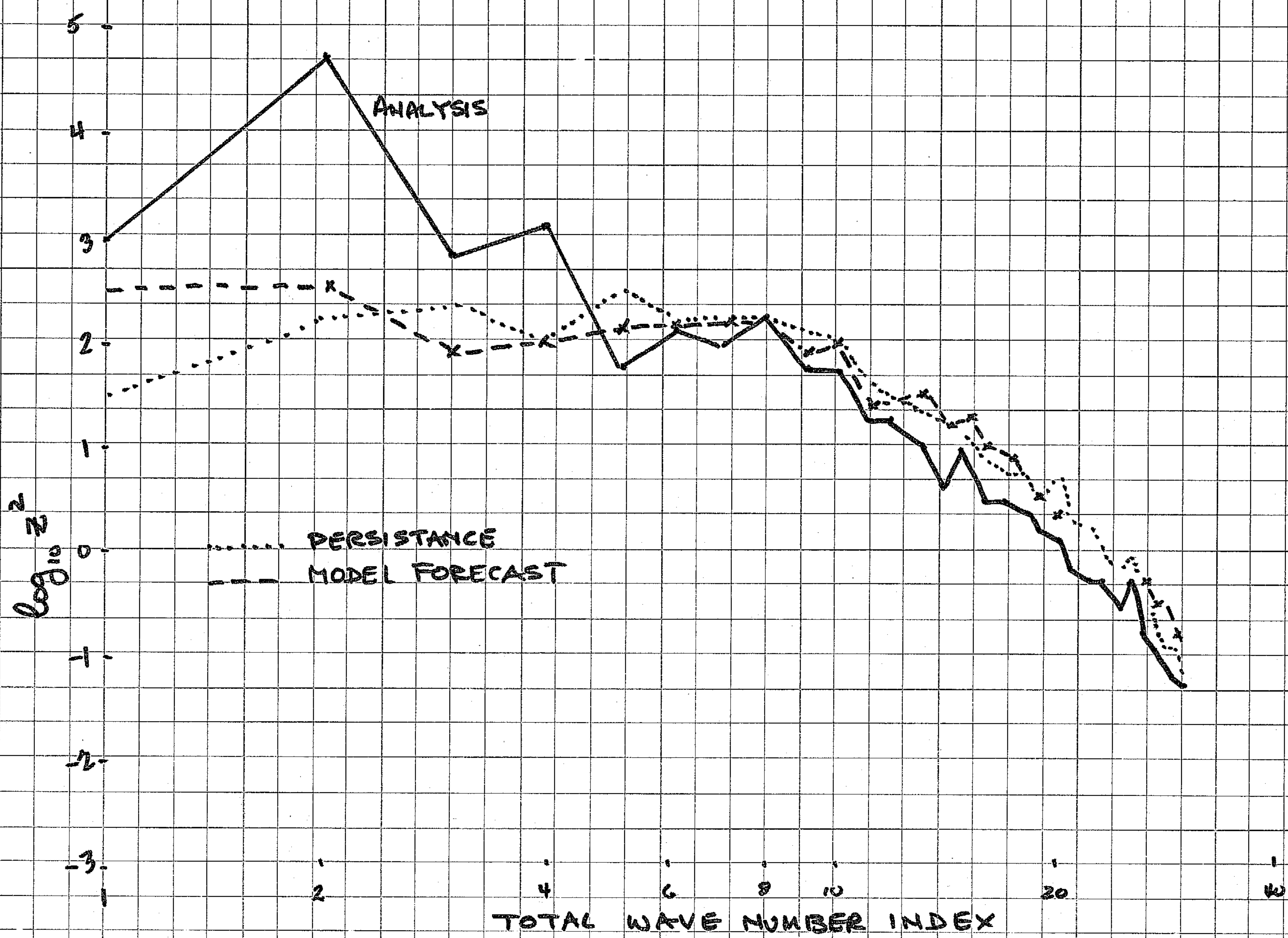

FIG 15 192 HR FORECAST ERROR